Research Article | Vol. 27, No. 10 | 13 May 2019 | OPTICS EXPRESS 13596
Optics EXPRESS

Grating monochromator wavelength calibration using an echelle grating wavelength meter

ANDREAS BAUMGARTNER

DLR German Aerospace Center, Münchener Straße 20, 82234 Weßling, Germany
*andreas.baumgartner@dlr.de

Abstract: Monochromators are a common utility for the spectral calibration of spectrometers. To guarantee traceability of characterization measurements to SI-standards, monochromators used as secondary standards must be properly calibrated. Common calibration procedures are based on the measurement of spectral lines emitted by gas-discharge lamps or lasers. Due to the nature of these light sources, the sampling of calibration points cannot be freely chosen. In this paper we present an approach where an echelle grating wavelength meter (WM) is used to traceably calibrate the emitted center wavelength of a monochromator at almost any sampling interval. In addition, it is possible to calibrate the monochromator outside the sensitive spectral range of the WM used. It is demonstrated how a WM is calibrated and then how it is used to calibrate the monochromator of DLR's Calibration Home Base (CHB) for imaging spectrometers at DLR Oberpfaffenhofen, Germany. The same approach is also used for the monochromator, which is intended for the laboratory calibration of the German hyperspectral satellite mission EnMAP.

1. Introduction

Monochromators are a widely used tool for the spectral calibration of spectrometers. Traceable monochromator calibration is essential for this application. Common monochromator calibration procedures involve replacing the light source with a gas-discharge lamp emitting known spectral lines as the standard [1, 2]. By tuning a monochromator's wavelength setting and simultaneously measuring the emitted power with a radiometer, the relation between grating angle and output wavelength is determined. The disadvantage of this approach is that a statement about the actual output wavelength can only be made at the positions of the spectral emission lines. This problem can be solved by an additional calibration of the electromechanical drive of a monochromator [3]. However, these types of measurements are not trivial and often cannot be easily carried out with commercially available systems. Schwarzmaier et. al. [4] showed that an echelle grating wavelength meter (WM) can be used for monochromator calibration.

In this paper we present a refinement of this method, which allows to tractably calibrate a grating monochromator at almost any sampling interval with an echelle grating WM. Additionally, it is possible to calibrate a monochromator beyond the sensitive range of the WM used.

This approach is used on a regular basis to calibrate the monochromator of DLR's Calibration Home Base (CHB) for imaging spectrometers at DLR Oberpfaffenhofen, Germany [5, 6]. It therefore has a direct influence on the spectral calibration of the airborne imaging spectrometers APEX (the Airborne Prism EXperiment) [7] and DLR's HySpex system [8], which are calibrated in this laboratory. Furthermore, the same approach and WM is used to calibrate the monochromator which is part of the ground support equipment of the German satellite mission EnMAP [9]. For both monochromators, the target uncertainty is ±0.1 nm in the VNIR and ±0.2 nm in the SWIR region.

The methods we describe were developed for a WM of type LambdaScan-usb distributed by GWU (GWU-Lasertechnik Vertriebsges.mbH) [10] but may apply for other instruments as well.

This paper is structured as follows: First we describe the functional principle of WMs and

#356087 https://doi.org/10.1364/OE.27.013596
Journal © 2019 Received 15 Jan 2019; revised 10 Mar 2019; accepted 13 Mar 2019; published 29 Apr 2019

Optics EXPRESS

the basic evaluation method for the general application of the measurement of monochromatic light. Then we discuss a method to use higher diffraction orders of a monochromator to calibrate its wavelength setting outside the sensitive spectral range of the WM. Finally, the traceable calibration of the LambdaScan-usb WM and how we use it to calibrate the CHB monochromator is presented.

2. Echelle grating wavelength meter

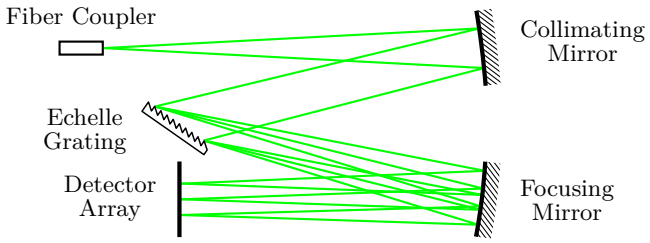

Fig. 1. Working principle of an echelle grating wavelength meter. Collimated light is diffracted by an echelle grating. Most of the energy is distributed to high diffraction orders which are imaged on a line detector array.

A WM is an optical instrument which measures the wavelength of monochromatic light. The operating principle of a WM that uses an echelle grating as dispersing element is shown in Fig. 1. A mirror creates a collimated beam from monochromatic light coming from an aperture - in the depicted case an optical fiber. This beam is then dispersed by an echelle grating and imaged by another mirror on a line detector array [11]. All these components remain fixed and no parts move. The optical properties of reflective echelle gratings are described by the grating equation

$$o\lambda = d\left(\sin(\theta) + \sin(\phi)\right), \tag{1}$$

with d as the grating constant, o the order of diffraction, λ the diffracted wavelength and θ and ϕ as the incident and diffraction angle, respectively. Echelle gratings are optimized to distribute more power to higher diffraction orders than conventional gratings. This enables the simultaneous imaging of several high diffraction orders of a monochromatic beam on a line detector array.

According to Eq. (1) and when all wavelength dependent properties of a WM are ignored, such as transmissivity, reflectivity and detector quantum efficiency, the imaged light of wavelength λ diffracted by the echelle grating by order o^{E} appears at the same position on the detector array as light of wavelength λ^{S} diffracted by order one,

$$\lambda^{\mathrm{S}} = \lambda \cdot o^{\mathrm{E}}, \qquad o^{\mathrm{E}} \in \mathbb{N}, \tag{2}$$

where the superscript “E” stands for echelle grating. Since the limitations ignored before apply to real instruments, light of diffraction order one is usually not detectable, because diffraction orders are typically in the range of 10 to 100. Therefore, we refer to the wavelength λ^{S} as synthetic wavelength in the following. Due to the high diffraction orders, small changes in the input wavelength result in big changes on the detector array. This means, that the resolution is magnified by the diffraction order.

The actual detectable input wavelength λ is limited by the sensitive spectral range of the WM,

$$\lambda^{\mathrm{E}}_{\mathrm{min}} \leq \lambda \leq \lambda^{\mathrm{E}}_{\mathrm{max}}, \tag{3}$$

which is usually given by the quantum efficiency of the detector. Each detector pixel is assigned a synthetic wavelength λ^{S} in the range of the minimum and maximum synthetic wavelength,

$$\lambda^{\mathrm{S}}_{\mathrm{min}} \leq \lambda^{\mathrm{S}} \leq \lambda^{\mathrm{S}}_{\mathrm{max}}, \tag{4}$$

which is determined by the optical layout of the WM. Creating a model for the relation between pixel number and synthetic wavelength is the purpose of the instrument calibration, see section 5.

A typical response caused by monochromatic light is shown in Fig. 2a. From Eq. (2) it follows, that the distance between adjacent synthetic wavelengths is equal to the actual wavelength λ

$$\lambda = \lambda^{\mathrm{S}}_{i+1} - \lambda^{\mathrm{S}}_{i}, \qquad i = 1, ..., n-1, \tag{5}$$

where n it the number of detected synthetic wavelengths.

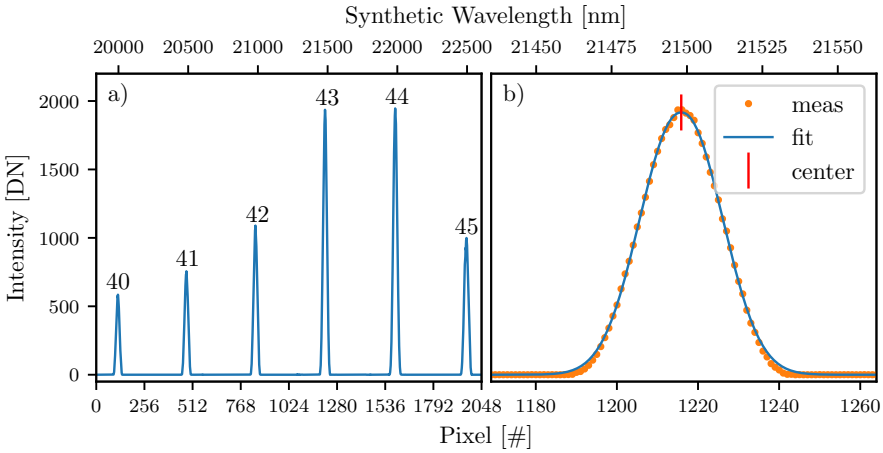

Fig. 2. Example of a measurement of monochromatic light with a wavelength of approximately 500 nm. a) Image acquired by a line detector array. The numbers next to the peaks are indicating the diffraction orders. b) Close up of peak four (diffraction order 43) with a fitted generalized Gaussian distribution function to determine the peak's center position. Light of 500 nm diffracted with order 43 results in a synthetic wavelength of 21 500 nm. The small deviation of the peak center shows that the actual wavelength is a bit smaller.

3. Measurement of monochromatic light

The methods described in this section are based on [10] and describe how WM detector readings are evaluated to determine the wavelength of monochromatic light, which is the common use case. As Fig. 2 shows, monochromatic light causes peak responses distributed over a line detector array. Contrary to the approach from [10], we fit a generalized Gaussian distribution function Γ to the data points z to determine the center of each peak in pixel coordinates x_i. In comparison to an ordinary Gaussian function, the generalized version represents the shape of the measured diffraction peaks more precisely, as the exponent is additionally parameterized:

$$\Gamma(z) = A \exp\left(-\left(\frac{|z-x|}{\alpha}\right)^{\beta}\right) \tag{6}$$

A detector signal is treated as a peak if the signal of one or more pixels is above a certain threshold value and if the signal on both sides of the maximum falls below another threshold value. By using the instrument calibration function f, see section 5, the pixel coordinates are converted to synthetic wavelengths λ^{S}_i:

$$\lambda^{\mathrm{S}}_i = f(x_i) \tag{7}$$

Optics EXPRESS

With help of Eq. (5) an approximation of the actual wavelength $\lambda^{\approx}$ can then be calculated by determining the average of the distances between the peak responses λ_i^{S}:

$$\lambda^{\approx} = \frac{1}{n-1} \sum_{i=1}^{n-1} \left(\lambda_{i+1}^{\mathrm{S}} - \lambda_i^{\mathrm{S}} \right) \tag{8}$$

With this information the diffraction orders o_i^{E} are calculated by dividing the synthetic wavelength λ_i^{S} with the approximated wavelength $\lambda^{\approx}$:

$$o_i^{\mathrm{E}} = \mathrm{round} \left(\lambda_i^{\mathrm{S}} / \lambda^{\approx} \right) \tag{9}$$

The quotient is rounded as diffraction orders must be natural numbers. Finally, the center wavelength of the input spectrum is determined by

$$\overline{\lambda} = \frac{1}{n} \sum_{i=1}^{n} \lambda_i^{\mathrm{S}} / o_i^{\mathrm{E}}. \tag{10}$$

Due to the rounding in Eq. (9), the uncertainty of approximated wavelength $\lambda^{\approx}$ has no influence on the final result. By dividing the synthetic wavelengths λ_i^{S} by the diffraction orders o_i^{E} the measurement uncertainties $\mathrm{u}(\lambda_i)$ are reduced by the same factor:

$$\mathrm{u}(\lambda_i) = \mathrm{u}(\lambda_i^{\mathrm{S}}) / o_i^{\mathrm{E}} \tag{11}$$

This means, that the higher the diffraction order, the lower is the uncertainty. Weighting the contributions to the calculated average in Eq. (10) with their uncertainties from Eq. (11) would be possible, but has due the high values of the diffraction orders o_i^{E} usually a minor influence on the result.

4. Monochromator calibration method

Though the principal evaluation method from section 3 can be used to calibrate a monochromator, the calibration range is limited to the sensitive spectral range of the WM. This limitation can be bypassed by measuring the higher diffraction orders of a monochromator, which are usually suppressed by spectral filters. Hence, these filters must be removed during calibration or, ideally, replaced by a glass window of the same thickness as the filters to minimize focus shifts along the optical axis. Usually, the order sorting filters are arranged in a rotary wheel, whereby one position is either kept empty or holds a window. In this case, a modification of the setup is not required. The effect of the focus shift is generally negligible, but can be verified by comparing the mean output wavelengths of measurements with and without windows or filters installed. Allowing higher diffraction orders to exit the monochromator also means that more than one wavelength is measured by the WM. Therefore, the usual evaluation method from section 3 does not work any more. An alternative method to determine the set wavelength is described in this section.

Figure 3 shows the schematic drawing of a monochromator setup where the emitted light from a broadband source, e.g. halogen lamp, is filtered by a monochromator and coupled into a multi-mode fiber. As it is depicted, the exit slit cuts out a region of the dispersed image of the entrance slit. Since the wavelength of the dispersed image changes continuously perpendicular to the exit slit, the wavelength of the emitted light changes in the same manner within the exit slit. This can lead to a possible spatial and angular dependence of the mean wavelength at the end of the fiber. For this reason, a mode scrambler is used here to create a uniform output spectrum. To measure the emitted wavelength, a WM is connected via the fiber to fiber coupler.

Optics EXPRESS

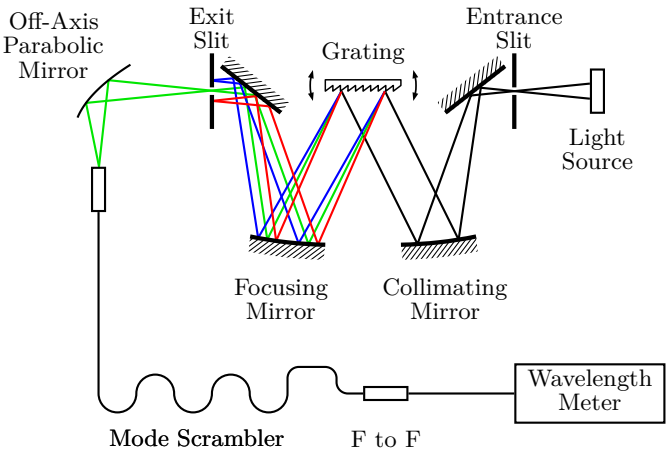

Fig. 3. Schematic drawing of a monochromator setup. The emitted light from a monochromator is coupled into a multi-mode fiber. Since the light has a certain bandwidth with changing wavelength over the exit port, a mode scrambler is used here to mix the modes in the fiber to create a uniform output spectrum. A fiber to fiber (F to F) coupler provides a modular interface to which a wavelength meter is connected. For the calibration measurements higher diffraction order suppressing filters are not placed in the optical path.

4.1. Higher monochromator diffraction orders

According to Eq. (1), the grating equation, in addition to the first order diffracted light $\lambda^{\mathrm{M}}(o^{\mathrm{M}} = 1)$, light of higher diffraction orders is also emitted by a monochromator, if there is no spectral filter in the optical path. The wavelength λ_j^{M} of this additional light is a fraction of the first order wavelength,

$$\lambda_j^{\mathrm{M}} = \frac{\lambda^{\mathrm{M}}(o^{\mathrm{M}} = 1)}{o_j^{\mathrm{M}}} \qquad j = 1, ..., m. \tag{12}$$

The wavelengths of the emitted spectrum λ_j^{M} must be within the spectral range of the monochromator:

$$\lambda_{\mathrm{min}}^{\mathrm{M}} \leq \lambda_j^{\mathrm{M}} \leq \lambda_{\mathrm{max}}^{\mathrm{M}} \tag{13}$$

Based on Eq. (12), the wavelength $\lambda^{\mathrm{M}}(o^{\mathrm{M}} = 1)$ of the emitted light which is diffracted by order one can be measured indirectly by measuring light diffracted by higher orders. This phenomenon can be used to calibrate wavelength settings of monochromators which are above the sensitive wavelength range of a WM if the wavelength of a higher order of diffraction is in the sensitive range.

When the light from a monochromator consisting of wavelengths λ_j^{M} is coupled into a WM, this light is diffracted again by the echelle grating as described in section 2. This twice diffracted light is then detected as the synthetic wavelengths λ_i^{S} with the WM diffraction orders o_i^{E}, which have the property

$$\lambda_i^{\mathrm{S}} / o_i^{\mathrm{E}} \in \lambda_j^{\mathrm{M}} \,. \tag{14}$$

Figure 4 shows an example of the measurement signal caused by monochromator light consisting of several different diffraction orders. Because each monochromator wavelength is a fraction of the order one wavelength, the diffraction on the echelle grating causes these wavelengths to overlap at certain peaks, a superposition of these wavelengths.

Optics EXPRESS

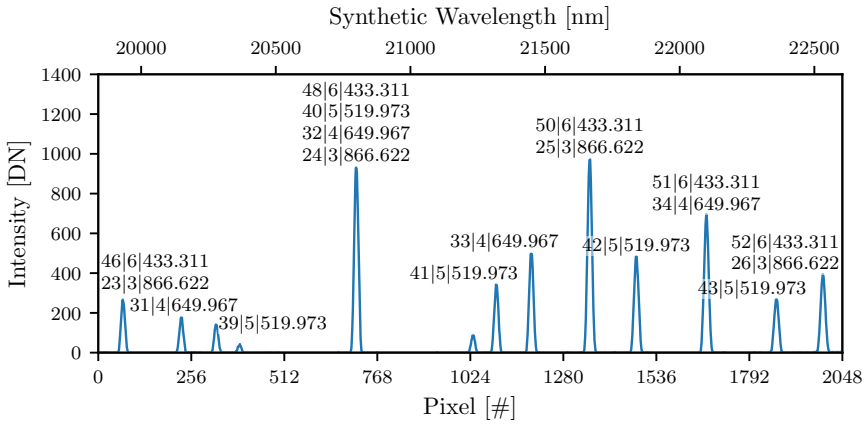

Fig. 4. Measurement with monochromator wavelength set to approximately 2600 nm. The values next to the peaks are indicating the wavelength meter diffraction orders, the monochromator diffraction orders and the emitted monochromator wavelengths in nm. The light of different wavelengths overlaps at several peaks. At one peak all wavelengths overlap. We refer to this peak as super peak.

4.2. *Superposition of all emitted wavelengths*

Since light from a monochromator can be composed of several different wavelengths, a rough estimation of the actual wavelength using the distances of adjacent peaks by Eq. (8) is not possible, see Fig. 4. However, according to Eq. (12), the first order diffracted light $\lambda_1^{\mathrm{M}}(o^{\mathrm{M}} = 1)$ is a multiple of all emitted monochromator wavelengths. A multiple of λ_1^{M} itself is sensed by the WM if

$$\lambda_1^{\mathrm{M}} < \lambda_{\mathrm{max}}^{\mathrm{S}} - \lambda_{\mathrm{min}}^{\mathrm{S}}. \tag{15}$$

In other words, there is one synthetic wavelength, a superposition, where all λ_j^{M} overlap, see Fig. 4. This peak - referred to as super peak in the following -, is identified by the procedures described below and is then used to identify the basic wavelengths of all other peaks.

To identify the super peak in the measured synthetic wavelengths λ_i^{S}, we assume that each synthetic wavelength λ_i^{S} is a multiple of λ_1^{M} and that this wavelength can be sensed by the WM. At first we calculate the potential WM diffraction orders by

$$o_i^{\mathrm{E,p}} = \mathrm{round}\left(\frac{\lambda_i^{\mathrm{S}}}{\lambda^{\star}}\right). \tag{16}$$

where $\lambda^{\star}$ is the coarse knowledge of the set monochromator wavelength which is in general available. Then we determine the potential basic wavelengths by

$$\lambda_i^{\mathrm{p}}(o^{\mathrm{M}} = 1) = \frac{\lambda_i^{\mathrm{S}}}{o_i^{\mathrm{E,p}}}. \tag{17}$$

Finally, we identify the index I of the correct wavelength in λ_i^{S} by determining which wavelength λ_i^{p} is closest to the initially guessed wavelength $\lambda^{\star}$ via

$$I = \arg\min_{\mathrm{i}} \left|\lambda_i^{\mathrm{p}} - \lambda^{\star}\right|, \tag{18}$$

where the wavelength of diffraction order 1 emitted by the monochromator is then

$$\lambda_1^{\mathrm{M}} = \lambda_I^{\mathrm{p}}. \tag{19}$$

It is possible that more than one super peaks exit. In this case, the approach does not change and one of these peaks is correctly identified as a super peak by Eq. (18). This also applies if only one wavelength is emitted by the monochromator.

As the choice of the correct peak in the WM spectrum as super peak and the determination of its diffraction order depends on the originally estimated wavelength $\lambda^\star$, the estimate must be accurate up to a certain amount. If the error of the guessed wavelength is too big, a peak next to the true super peak or the diffraction order is wrongly chosen. It is obvious, that the synthetic wavelengths next to the super peak $\lambda_{I\pm1}^{\mathrm{S}}$ cannot be closer than the shortest emitted wavelength $\lambda_{\mathrm{min}}^{\mathrm{M}}$. Since the error is magnified by the WM diffraction order o_I^{E}, the error must be less than half of the shortest emitted wavelength divided by the WM diffraction order

$$e(\lambda^\star) < 0.5\frac{\lambda_{\mathrm{min}}^{\mathrm{M}}}{o_I^{\mathrm{E}}}, \qquad o_I^{\mathrm{E}} = \frac{\lambda_I^{\mathrm{S}}}{\lambda_I^{\mathrm{M}}}. \tag{20}$$

4.3. Determination of the basic wavelength of the remaining peaks

Although, the set monochromator wavelength λ_1^{M} is already known, examining the other peaks of the WM measurement increases the precision. With the knowledge that at index I of the synthetic spectrum λ_i^{S} is a superposition of all the wavelengths of the emitted monochromator spectrum λ_j^{M}, the basic wavelengths of the other synthetic wavelengths can be determined. The distance from the super peak λ_I^{S} to each other peak in the synthetic spectrum λ_i^{S} must be an integer multiple of a wavelength present in the emitted monochromator spectrum λ_j^{M}.

At first, we determine the emitted monochromator spectrum λ_j^{M} with the help of Eq. (12), where the possibly emitted and detected diffraction orders o_j^M are calculated by

$$o_j^M = 1, ..., \mathrm{round}\left(\frac{\lambda_1^{\mathrm{M}}}{\max\left(\lambda_{\mathrm{min}}^{\mathrm{E}}, \lambda_{\mathrm{min}}^{\mathrm{M}}\right)}\right). \tag{21}$$

Then the ratios of the distances of each synthetic wavelength to the super peak $\left|\lambda_i^{\mathrm{S}} - \lambda_I^{\mathrm{S}}\right|$ divided by each monochromator wavelength λ_j^{M} is obtained by

$$R_{ij} = \frac{\left|\lambda_i^{\mathrm{S}} - \lambda_I^{\mathrm{S}}\right|}{\lambda_j^{\mathrm{M}}}. \tag{22}$$

The indexes of the ratios which are closest to integer numbers are identified by

$$J_i = \arg\min_j \left|R_{ij} - \mathrm{round}(R_{ij})\right|, \tag{23}$$

where the corrected corresponding monochromator wavelength is then $\lambda_{J_i}^{\mathrm{M}}$ and the monochromator diffraction orders are $o_{J_i}^M$. Finally, we use each wavelength in the spectrum λ_i^{S} for the determination of λ_1^{M} and increase therefore its precision:

$$\lambda_1^{\mathrm{M}} = \frac{1}{n}\sum_{i=1}^{n} \frac{\lambda_i^{\mathrm{S}}}{\mathrm{round}\left(\lambda_i^{\mathrm{S}}/\lambda_{J_i}^{\mathrm{M}}\right)} \cdot o_{J_i}^M \tag{24}$$

Optics EXPRESS

5. Echelle grating wavelength meter calibration methods

The calibration of a WM is usually performed by measuring well known spectral lines emitted by gas-discharge lamps or lasers.

5.1. Calibration polynomial

From N^{ref} measurements of reference wavelengths λ_k^{ref} originate a number of measured peaks of synthetic wavelengths $\lambda_{kl}^{\mathrm{S,ref}}$

$$\lambda_{kl}^{\mathrm{S,ref}} = \lambda_k^{\mathrm{ref}} o_{kl}^{\mathrm{E}}, \qquad k = 1, ..., N^{\mathrm{ref}}, \qquad l = 1, ..., N_k^{\mathrm{ref,S}}, \tag{25}$$

where $N_k^{\mathrm{ref,S}}$ is the number of synthetic wavelengths which result from reference wavelength λ_k^{ref}. We derive the center of each peak in pixel coordinates x_i by fitting a generalized Gaussian distribution function, see section 3. The corresponding synthetic wavelength is then the product of its reference wavelength λ_i^{ref} and the diffraction order o_i^{E}

$$\lambda_{kl}^{\mathrm{S,ref}} = \lambda_k^{\mathrm{ref}} o_{kl}^{\mathrm{E}}, \tag{26}$$

where m is the number of synthetic wavelengths. The diffraction orders o_{kl}^{E} are derived similarly to Eq. (9). A coarse knowledge of a peak's synthetic wavelength $\lambda^{\mathrm{S},\approx}$ can either be derived from an existing but maybe outdated calibration or from the instrument geometry. Eq. (9) changes then to

$$o_{kl}^{\mathrm{E}} = \mathrm{round}\left(\lambda_{kl}^{\mathrm{S},\approx} / \lambda_k^{\mathrm{ref}}\right). \tag{27}$$

Accordingly, the uncertainty of the synthetic reference wavelength is the product of the uncertainty of the reference wavelength and the diffraction order:

$$u(\lambda_{kl}^{\mathrm{S,ref}}) = u(\lambda_k^{\mathrm{ref}}) o_{kl}^{\mathrm{E}} \tag{28}$$

A polynomial function f with coefficients c is then fitted to derive a model for the relation of pixel coordinates to synthetic wavelengths

$$c^{\mathrm{calib}} = \arg\min_c \sum_{k=1}^{N^{\mathrm{ref}}} \sum_{l=1}^{N_k^{\mathrm{ref,S}}} \left(f_c(x_{kl}) - \lambda_k^{\mathrm{ref}} o_{kl}^{\mathrm{E}}\right)^2, \tag{29}$$

where c^{calib} are the optimized coefficients.

5.2. Update of wavelength meter calibration

When an optical fiber is attached to a WM, the position of the fiber core might differ to the one during calibration. To create new calibration coefficients (as described in section 5.1) each time a fiber is attached would be too time consuming. Therefore, we only update the offset value of the calibration coefficients c_0^{calib} of the WM by measuring one reference wavelength.

For each measured peak, we derive the synthetic wavelength λ^{S} with the existing calibration coefficients c^{calib} as well as its diffraction orders o_i^{E}. The offset between evaluated synthetic wavelengths λ_i^{S} and expected synthetic wavelengths $\lambda^{\mathrm{ref,air}} o_i^{\mathrm{E}}$ is used to update c_0^{calib} of the calibration polynomial:

$$c_0^{\mathrm{updated}} = c_0^{\mathrm{calib}} - \frac{1}{n} \sum_{i=1}^{n} \left(\lambda_i^{\mathrm{S}} - \lambda^{\mathrm{ref,air}} o_i^{\mathrm{E}}\right) \tag{30}$$

Optics EXPRESS

6. Wavelength meter calibration measurements

6.1. Instrument

For the calibration of the CHB and the EnMAP calibration monochromators, we use a WM of type LambdaScan-usb distributed by GWU (GWU-Lasertechnik Vertriebsges.mbH). Some of the vendor's specifications of the WM, see Table 1, are only valid when the software supplied with the instrument is used. For the evaluation approach proposed in section 4 the *accuracy*, *source linewidth requirement* and *resolution* do not apply. A fourth order calibration polynomial was supplied with the instrument which was created during factory calibration. Throughout the course of measurements the same optical fiber stayed connected to the WM.

Table 1. Specifications of the wavelength meter LambdaScan-usb [10]. Note: The specifications for *accuracy*, *source linewidth requirement* and *resolution* only apply when the software supplied with the instrument is used, not for the approach stated in section 4.

Parameter	Value
Measurement range	240 nm to 1250 nm
Resolution $\Delta\lambda/\lambda$, better than	$\sim 5 \times 10^{-5}$ ($\sim$3 cm^{-1} @ 500 nm)
Accuracy $u(\lambda)/\lambda$	$\sim 5 \times 10^{-5}$ ($\pm$0.0125 nm @ 500 nm)
Source linewidth requirement	$\leq$ 150 cm^{-1}
Number of channels	2048

6.2. Full instrument calibration measurements

Because we fit an analytical function on the data points, see section 3, in contrast to the method used by the supplied software, we create new calibration coefficients. As wavelength reference we use 17 emission lines of a neon discharge lamp, see Table 2. We place the lamp as light source in front of the monochromator as it is shown in Fig. 3 and connect the optical fiber of the WM to the optical fiber of the monochromator setup. We use the monochromator as a tunable filter to select single emission lines and suppress all others. For this use case, the wavelength accuracy of the monochromator has no influence on the wavelength of the output spectrum. Before we start the measurements, we record temperature, pressure and humidity with a calibrated weather station.

6.3. Repeatability

To evaluate the stability of the WM, we repeat the measurements described in section 6.2 three, four and five days apart from the initial calibration measurements and recorded the environmental parameters in the same manner.

6.4. Calibration update measurements

To avoid a complete recalibration of the WM each time a fiber is attached, we measure a single emission line to update an existing calibration polynomial, see section 5.2. As reference source we use the spectral emission line of a mercury discharge lamp with a vacuum wavelength of 435.956 13 nm [12]. We place a bandpass filter between lamp and fiber to suppress all other emission lines, see Fig. 5. To ensure that the light coupled from the fiber into the WM is uniformly distributed, we put together the fiber entrance, the filter and the lamp as close as possible, so that the numerical aperture of the optical fiber is overfilled.

We performed this measurement before the calibration measurements described in section 6.2 to evaluate the influence on the instrument model.

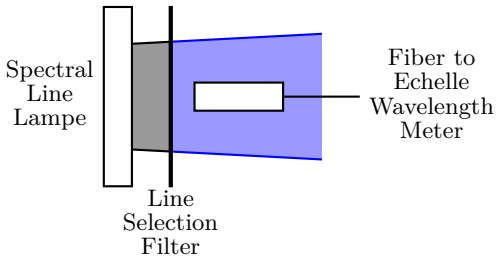

Fig. 5. Setup for wavelength meter calibration update measurements. A spectral bandpass filter is placed between a gas-discharge lamp and the multi-mode fiber leading to the WM. A fiber connector is symbolized by the white box attached to the fiber. The filter suppresses all emission lines but one. The components are packed together as closely as possible to guarantee overfilling of the fiber's numerical aperture.

7. Wavelength meter calibration results

7.1. Wavelength in air

To calculate the wavelengths in air for the neon and mercury emission lines, we took the vacuum wavelength λ^{vac} provided by the NIST Atomic Data Base [12]. We corrected these for the refractive index of air n^{air} according to the formula of [13]:

$$\lambda^{\mathrm{air}} = \frac{\lambda^{\mathrm{vac}}}{n^{\mathrm{air}}(T, p, h, x_c)}, \tag{31}$$

where T is the temperature, p the pressure, h the humidity and x_c the CO_2 content. The temperature was between 292.2 and 292.6 K measured with an uncertainty of 0.3 K, the pressure was between 93200 and 94 380 Pa recorded with an uncertainty of 155 Pa and the humidity varied from 27 to 35 % with a measurement uncertainty of 1.1 %. We assume that the CO_2 was (450 ± 75) ppm. All parameters remained stable during the measurements. The vacuum wavelengths of the emission lines we used and the calculated wavelengths in air with their uncertainties are pointed out in Table 2. The dominant uncertainties for the refractive indexes and the wavelengths in air originate in the uncertainties of the environmental parameters. In comparison, the uncertainty of the refractive index model [13] and the uncertainties of the vacuum wavelengths are negligible.

7.2. Results of full calibration

From the 17 neon emission lines that we used as the calibration standard originated 66 synthetic wavelengths. The calibration coefficients were then created according to section 5.1. We derived the diffraction orders o_i^{E} of each synthetic wavelength by using Eq. (27) along with the existing manufacturer's calibration. We then fitted a fourth order polynomial to the data points.

The residuals between the calibration polynomial and the synthetic neon wavelengths are shown in Fig. 6. It can be seen, that the uncertainties of the reference wavelengths are negligible compared to the deviations from the model. The data points are well distributed over the whole synthetic wavelength range, demonstrating that the emission lines used are sufficient to get a proper fit result.

Optics EXPRESS

Table 2. Wavelengths in vacuum and air of the neon and mercury emission lines used for calibration. The vacuum wavelengths [12] are corrected for the refractive index of air [13]. The neon lamps were used on four different days with different environmental parameters, where at $\Delta t = 0\,\mathrm{d}$ we performed the calibration measurements and on the three other days the repeatability tests. The given uncertainties for the wavelengths in air originate in the uncertainties of the environmental parameters.

Lamp	$\lambda^{\mathrm{vac}}[nm]$	$\lambda^{\mathrm{air}}[nm]$ $\Delta t = 0\,\mathrm{d}$	$\lambda^{\mathrm{air}}[nm]$ $\Delta t = 3\,\mathrm{d}$	$\lambda^{\mathrm{air}}[nm]$ $\Delta t = 4\,\mathrm{d}$	$\lambda^{\mathrm{air}}[nm]$ $\Delta t = 5\,\mathrm{d}$	$u(\lambda^{\mathrm{air}})[nm]$
Hg	435.95613	435.84372	N.A.	N.A.	N.A.	0.00022
Ne	585.41102	585.26216	585.26402	585.26276	585.26417	0.00029
Ne	594.64812	594.49699	594.49888	594.49760	594.49903	0.00029
Ne	607.60194	607.44762	607.44955	607.44825	607.44970	0.00030
Ne	609.78507	609.63022	609.63215	609.63084	609.63230	0.00030
Ne	616.52996	616.37345	616.37541	616.37408	616.37556	0.00030
Ne	621.90013	621.74230	621.74427	621.74293	621.74442	0.00031
Ne	626.82283	626.66378	626.66577	626.66442	626.66593	0.00031
Ne	630.65325	630.49326	630.49526	630.49390	630.49542	0.00031
Ne	633.61793	633.45721	633.45922	633.45786	633.45938	0.00031
Ne	650.83259	650.66763	650.66969	650.66829	650.66985	0.00032
Ne	653.46870	653.30309	653.30516	653.30376	653.30532	0.00032
Ne	668.01201	667.84281	667.84493	667.84349	667.84509	0.00033
Ne	671.88974	671.71958	671.72171	671.72027	671.72188	0.00033
Ne	693.13788	692.96248	692.96467	692.96319	692.96484	0.00034
Ne	717.59155	717.41011	717.41238	717.41084	717.41255	0.00035
Ne	724.71632	724.53312	724.53541	724.53385	724.53559	0.00036
Ne	744.09472	743.90672	743.90908	743.90748	743.90926	0.00037

7.3. Results of repeatability measurements

The results of the repeatability measurements along with the calibration measurements and the results from the vendor's software are shown in Fig. 7: the measurement results are five-times more accurate as originally specified by the manufacturer. We assume this is caused by the fact that we fit an analytical function on the measured peaks to retrieve the pixel position with subpixel resolution, see section 3, while the instrument specifications indicate that this is not the case for the supplied software. On average, the residuals are 0.0013 nm with a maximum deviation of 0.0031 nm.

7.4. Results of calibration update measurements

Applying the offset correction derived from of the mercury line measurements, see section 5.2, adds a bias of −0.0011 nm. Although, this bias can be reduced by measuring more emission

Optics EXPRESS

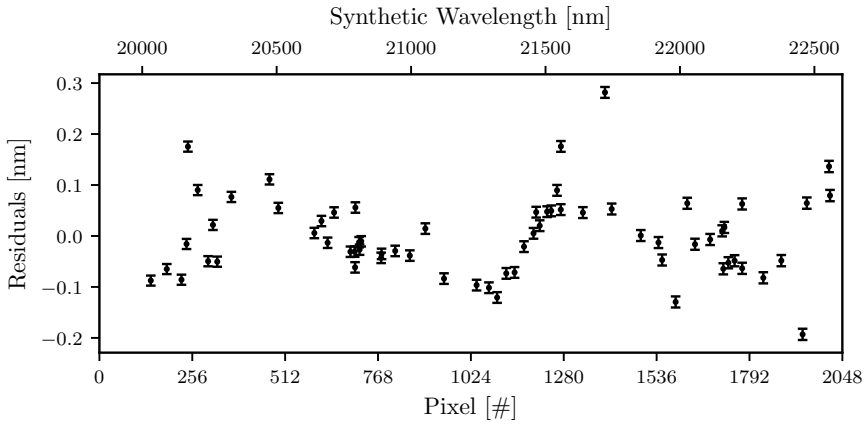

Fig. 6. Residuals between fitted calibration polynomial and reference wavelengths. The uncertainties, which are dominated by the uncertainties of the environmental parameters, are negligible compared to the deviations. Note: These are the residuals for the synthetic wavelengths, not for the actually measured wavelengths.

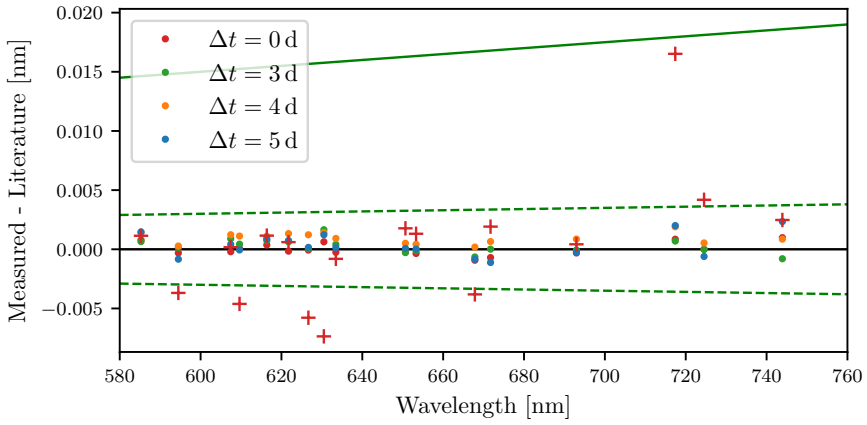

Fig. 7. Result of the stability assessment by repeated neon discharge lamp measurements. Dots denote the results of the evaluation approach presented in this paper, whereas the dashed lines are the derived uncertainty. Crosses represent the outcome of the software supplied with the instrument with the solid line as the uncertainty specified by the manufacturer.

lines, it is negligible for the intended use case, see section 8.

7.5. Derived measurement uncertainty

We derive a new measurement uncertainty for the WM from the experimental results from section 7.3. Thus all uncertainties of the measurement and evaluation process are taken into account and an additional treatment of the uncertainties is not necessary. Since the validation measurement consist of only four data takes with different environmental conditions, we conservatively define

Optics EXPRESS

a new measurement uncertainty of

$$\frac{u(\lambda)}{\lambda} = 5 \cdot 10^{-6}; (k = 1). \tag{32}$$

Even adding the bias from the calibration update measurements, the residuals from the neon discharge lamp measurements are below this uncertainty.

8. Monochromator calibration measurements

In this section exemplary calibration results of the CHB monochromator of type MS257 from Oriel, distributed by Newport, are shown. The monochromator (asymmetrical Czerny-Turner design) is equipped with three different gratings, optimized for the wavelength range of 400 to 2500 nm, see Table 3. For a 1200 l/mm grating at 553 nm the accuracy is specified with 0.1 nm, <0.15 nm max; the repeatability is 0.015 nm, <0.03 nm max. With 600 l/mm gratings, these values approximately double.

Table 3. Specifications of the three installed gratings and the corresponding measurement parameters. λ_{min}, λ_{max} and $\Delta\lambda$ are the start, the end and the step width of the measurements, respectively.

Grating [#]	Line Density [l / mm]	Blaze Wavelength [nm]	λ_{min} [nm]	λ_{max} [nm]	$\Delta\lambda$ [nm]
1	1200	350	370	1100	1
2	1200	750	400	1200	1
3	600	1600	900	2600	2

We performed the calibration of the monochromator for all three gratings over the wavelength range from 370 to 2600 nm accordingly to Table 3. The monochromator setup is similar to the one shown in Fig. 3. The spectrum of a halogen lamp is coupled into the monochromator and the WM is connected to the fiber.

From these measurements we generated calibration tables for each grating. By linearly interpolating between the sampling points we corrected systematic monochromator errors of the second measurements. In this manner, we repeated the calibration measurements after four days to validate the correction of systematic errors and to investigate the stability of the monochromator.

9. Monochromator calibration results

Figure 8 shows the results of the calibration and validation measurements. The uncertainties of the WM measurements are negligible, since for a wavelength of 1000 nm the uncertainty is 0.005 nm and for 2500 nm it is 0.0125 nm, see section 7.

In the residuals of the calibration measurements a sinusoidal pattern can be seen which is caused by the worm drive turning the grating turret. Since this is not a statistical but systematic error it must be corrected. It is important to note, that the monochromator under investigation is more than 20 years old. Therefore, these results should not be misunderstood as an evaluation of the performance of this device series.

On the other side, the residuals of the validation measurements are within a range of ±0.1 nm. The original sinusoidal pattern vanished, but a short-term periodic fluctuation with small amplitudes remains. Since the remaining pattern does not correlate with the original one, we

assume that this is related to the repeatability of the stepper motor of the monochromator. A linear trend is visible in the residuals of grating 1, where the error decreases with increasing wavelengths. It seems, that we started the measurements before the monochromator was completely thermally stabilized. However, all residuals are within the desired uncertainty of ±0.1 nm, even for grating 3, where the target uncertainty is ±0.2 nm.

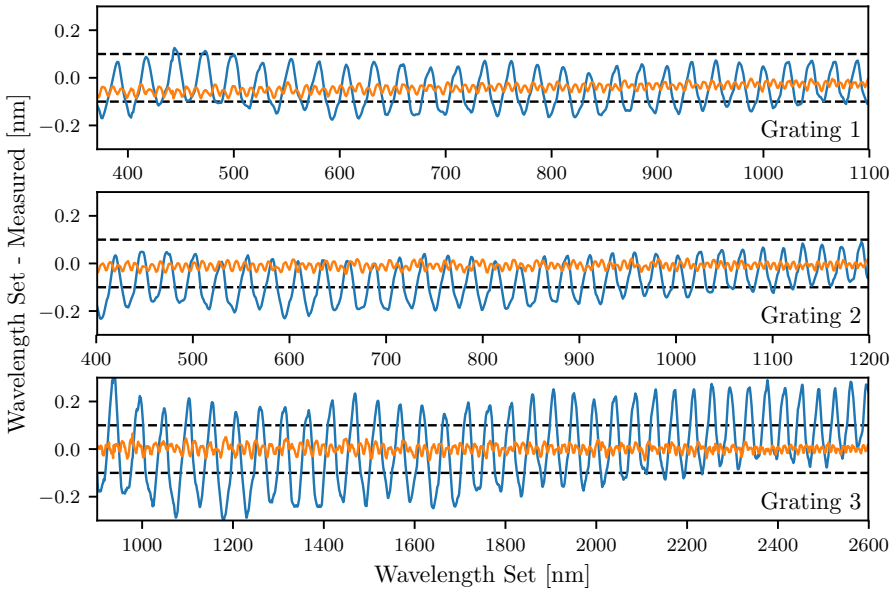

Fig. 8. Residuals of monochromator calibration (blue) and validation measurements utilizing the former calibration (orange) for all three gratings. A sinusoidal pattern can be seen in the calibration measurements, caused by the worm gear of the grating turret. The pattern vanished completely in the validation measurements.

10. Conclusion

In this paper we presented a method to calibrate grating monochromators with almost arbitrary sampling interval, traceable to gas-discharge lamps by using an echelle grating wavelength meter. The theoretical lower limit of the sampling interval results from the step size of the monochromator, since the WM enables continuous wavelength measurements. The approach allows the determination of the first diffraction order wavelength, even beyond the nominal sensitive spectral range of the wavelength meter used. This is done by removing a monochromator's spectral filters for higher diffraction order suppression and measuring multiple diffraction orders simultaneously. The approach allows the determination of the first diffraction order wavelength, even when several other orders are present. Further, monochromators can be calibrated beyond the sensitive spectral range of the used wavelength meter. We demonstrated the calibration and the assessment of the repeatability of an off-the-shelf echelle grating wavelength meter. It turned out, that the proposed evaluation approach is more than five times as accurate than using the software supplied with the instrument. With help of the wavelength meter we calibrated a monochromator which eliminated systematic errors leading to significant improvements of the precision of the emitted wavelengths. Due to the accuracy of the wavelength meter calibration, the measurement uncertainty is negligible for the monochromator calibration.

Optics EXPRESS

References

1. J. N. Miller, *Standards in fluorescence spectrometry* (Chapman and Hall, 1981).
2. W. D. Bare and J. N. Demas, "Monochromator wavelength calibration standards extending into the near-infrared using second- and third-order emission lines from mercury vapor lamps," J. Fluoresc. **10**, 317–324 (2000).
3. C. L. Hepplewhite, J. J. Barnett, K. Djotni, J. G. Whitney, J. N. Bracken, R. Wolfenden, F. Row, C. W. P. Palmer, R. E. J. Watkins, R. J. Knight, P. F. Gray, and G. Hammond, "Hirdls monochromator calibration equipment," Proc. SPIE **5152**, 205 (2003).
4. T. Schwarzmaier, A. Baumgartner, P. Gege, and K. Lenhard, "Calibration of a monochromator using a lambdameter," Proc. SPIE **8889**, 888910 (2013).
5. DLR Remote Sensing Technology Institute, "The calibration home base for imaging spectrometers," Journal of large-scale research facilities **2**, A82 (2016).
6. P. Gege, J. Fries, P. Haschberger, P. Schoetz, H. Schwarzer, P. Strobl, B. Suhr, G. Ulbrich, and W. Vreeling, "Calibration facility for airborne imaging spectrometers," ISPRS J. Photogramm. & Remote. Sens. **64**, 387–397 (2009).
7. M. E. Schaepman, M. Jehle, A. Hueni, P. D'Odorico, A. Damm, J. Weyermann, F. D. Schneider, V. Laurent, C. Popp, F. C. Seidel, K. Lenhard, P. Gege, C. Küchler, J. Brazile, P. Kohler, L. D. Vos, K. Meuleman, R. Meynart, D. Schläpfer, M. Kneubühler, and K. I. Itten, "Advanced radiometry measurements and earth science applications with the airborne prism experiment (apex)," Remote. Sens. Environ. **158**, 207–219 (2015).
8. DLR Remote Sensing Technology Institute, "Airborne imaging spectrometer hyspex," Journal of large-scale research facilities **2**, A93 (2016).
9. L. Guanter, H. Kaufmann, K. Segl, S. Foerster, C. Rogass, S. Chabrillat, T. Kuester, A. Hollstein, G. Rossner, C. Chlebek, C. Straif, S. Fischer, S. Schrader, T. Storch, U. Heiden, A. Mueller, M. Bachmann, H. Mühle, R. Müller, M. Habermeyer, A. Ohndorf, J. Hill, H. Buddenbaum, P. Hostert, S. van der Linden, P. LeitÃčo, A. Rabe, R. Doerffer, H. Krasemann, H. Xi, W. Mauser, T. Hank, M. Locherer, M. Rast, K. Staenz, and B. Sang, "The enmap spaceborne imaging spectroscopy mission for earth observation," Remote. Sens. **7**, 8830–8857 (2015).
10. *GWU LambdaScan-usb Technical Manual* (George Washington University, 2009), version 3.22 ed.
11. M. B. Morris and T. J. Mclirath, "Portable high-resolution laser monochromator-interferometer with multichannel electronic readout," Appl. Opt. **18**, 4145 (1979).
12. A. Kramida, Yu. Ralchenko, J. Reader, and and NIST ASD Team, "Nist atomic spectra database ver. 5.5.6," https://physics.nist.gov/asd (2018). Accessed: 2018-10-12.
13. P. E. Ciddor, "Refractive index of air: New equations for the visible and near infrared," Appl. Opt. **35**, 1566 (1996).